Studies on a Group of Silicon Carbide Structures

RICHARD S. MITCHELL*
Mineralogical Laboratory, University of Michigan, Ann Arbor, Michigan
(Received May 10, 1954)

Morphological and structural details of silicon carbide type 141*R* are given. This polymorph, having a structure represented by the zigzag sequence 3333333333333332, is a member of the '3...2' rhombohedral series proposed by Ramsdell [Am. Mineralogist **32**, 64 (1947)].

A detailed study of the '3...2' series is undertaken, resulting in an empirical mechanism which can be used for the direct determination of the structure of any member of this series. Using this means the structure of the new polymorph 393*R* is suggested.

INTRODUCTION

WITH the discovery of each new polymorph of silicon carbide it becomes more evident that there is no limit to the possible modifications of this substance. Up to the present time, the structures of 15 types have been established. The largest structure of this group is 87*R*.[1] Types consisting of a larger number of layers have also been reported, but no satisfactory analysis of their structures has so far been advanced. Some of these types are ~270*R*,[2] 594*R*[3]; 141*R*, 168*R*, 192*R*,[4] and recently the writer has also identified 120*R*, 393*R*, 33*H*, 48*H*, and three specimens of 78*H*. In this paper a structure for type 141*R* is proposed which is in good agreement with the observed data. Upon the basis of this new structure as well as from previously known structures, the writer suggests a mechanism for the direct determination of the structures of an evidently common group of silicon carbide polymorphs. Using this means the structure of type 393*R* is proposed. Much work has also been done on the structures of some of the other types listed above, but at present no definite results can be reported.

DISCOVERY AND IDENTIFICATION OF 141*R*

Two specimens of silicon carbide 141*R* have been encountered at this laboratory. The first of these (No. 109), upon which all the structural work was based, was discovered in 1950. Though the presence of this form was first noticed on Weissenberg films, its exact identity was not determined until later by the use of the Laue method. The second specimen (No. 169) was discovered recently during an investigation, with the Laue method, of a number of silicon carbide crystals showing growth spirals. The x-ray patterns of these two specimens are identical.

Both specimens of silicon carbide 141*R* are coalesced with type 6*H*. The 6*H* Laue spots are valuable reference points in the identification of this new rhombohedral form. In any rhombohedral type (*xR*), the *range* from 10·0 to 10·*x* for *xR* coincides exactly with the range 10·0 to 10·6 for 6*H*. One must remember, however, that the 10·*l* reflections of the rhombodhedral *xR* are missing when $l-1\neq 3n$. It also follows that the range between two adjacent 6*H* reflections, e.g., 10·1 to 10·2, coincides exactly with 1/6 of the 10·0 to 10·*x* range of *xR*. Thus, if 6*H* spots were present on a film with unknown *xR* spots, one could identify the *xR* type by multiplying by 6 the number of spaces between the *xR* 10·*l* reflections that lie between any two adjacent 6*H* 10·*l* spots, counting, of course, the spaces between the missing reflections caused by the rhombohedral lattice. On the x-ray films 23.5 of these spaces lie between the known 10·1 and 10·2 6*H* reflections. The number of layers in the unknown type would, therefore, be $6\times 23.5=141$. A synthetic Laue pattern of silicon carbide 141*R* was also constructed according to the method previously described.[5] This corresponded exactly with the 10·*l* spots on the Laue film.

THE STRUCTURE OF 141*R*

Those 141*R* 10·*l* reflections which coincide most closely with 6*H* 10·*l* positions are of stronger intensity. This intensity coincidence is an indication of the presence of many 33 units, which characterize 6*H*, in the zigzag sequence of 141*R*. Assuming that many 33 units are necessary because of this intensity distribution, and also that the only numbers found in zigzag sequences are 2, 3, and 4,[6] the only possible way to complete the 141*R* cell is the arrangement 3333333333333332. The calculations for this sequence gave satisfactory agreement with the observed intensities of the films. Table I compares the calculated and observed intensities for this sequence. Other evidence supporting the validity of this sequence for the 141*R* structure is presented in a later section.

This new rhombohedral polymorph has the following (hexagonal) cell dimensions:

$$a_0=3.073\ kX,\dagger \quad c_0=354.33_3\ kX, \quad Z=141$$

* Present address: Department of Geology, University of Virginia, Charlottesville, Virginia.

[1] L. S. Ramsdell, Am. Mineralogist **32**, 64 (1947).

[2] G. S. Zhdanov and Z. V. Minervina, J. Exptl. Theoret. Phys. **17**, 3 (1947).

[3] Honjo, Miyake, and Tomita, Acta Cryst. **3**, 396 (1950).

[4] L. S. Ramsdell and R. S. Mitchell, Am. Mineralogist **38**, 56 (1953).

[5] R. S. Mitchell, Am. Mineralogist **38**, 60 (1953).

[6] L. S. Ramsdell and J. A. Kohn, Acta Cryst. **5**, 215 (1952).

† These dimensions are given in *kX* units to agree with the earlier published data which, although reported as Angstrom units, were really in *kX* units.

or, for rhombohedral axes,

$$a_{rh}=118.12_4\,kX,\quad \alpha=1°30',\quad Z=47.$$

The space group for 141*R* is *R*3*m*, as in the other known rhombohedral polymorphs. The zigzag sequence 3333333333333332, which must be repeated three times to give the complete unit cell, results in the following atomic positions:

47 *Si* at 0, 0, *rz*
47 *C* at 0, 0, *rz*+*p*
47 *Si* and 47 *C* at 1/3, 2/3, 2/3+the above coordinates
47 Si and 47 *C* at 2/3, 1/3, 1/3+the above coordinates.
r=0, 2, 6, 8, 12, 14, 18...48; 51, 54, 57, 60...93; 97, 99, 103, 105, 109, 111, 115...139.
z=1/141
p=(3/4) (1/141).

TABLE I. Comparison of observed and calculated intensities for some of the reflections of type 141*R*.

(10.*l*)	I_{calc}	I_{obs}	(10.*l*)	I_{calc}	I_{obs}
10.1	0.8	vvw?	$10.\bar{3}\bar{5}$	0.4	a
4	0.9	vvw?	$\bar{3}\bar{8}$	3.2	a
7	2.0	vvw	$\bar{4}\bar{1}$	1.5	a
10	1.2	vvw	$\bar{4}\bar{4}$	0.1	a
13	8.0	vw	$\bar{4}\bar{7}$	1000.0	vvs
16	6.5	vw	$\bar{5}\bar{0}$	2.1	a
19	21.9	w	$\bar{5}\bar{3}$	2.4	a
22	190.3	ms	$\bar{5}\bar{6}$	0.0	a
25	129.9	ms	$\bar{5}\bar{9}$	5.0	a
28	30.0	mw	$\bar{6}\bar{2}$	0.0	a
31	23.9	w	$\bar{6}\bar{5}$	1.7	vvw
34	25.9	w	$\bar{6}\bar{8}$	18.3	w
37	12.0	w	$\bar{7}\bar{1}$	685.8	vs
40	17.0	w	$\bar{7}\bar{4}$	19.2	w
43	52.5	m	$\bar{7}\bar{7}$	0.1	vw
46	740.4	vs	$\bar{8}\bar{0}$	5.7	vw
49	139.3	ms	$\bar{8}\bar{3}$	12.9	vw
52	21.9	w	$\bar{8}\bar{6}$	5.2	vvw
55	14.9	vw	$\bar{8}\bar{9}$	14.1	w
58	2.9	vw	$\bar{9}\bar{2}$	78.0	m
61	6.4	vw	$\bar{9}\bar{5}$	221.3	ms
64	4.5	w	$\bar{9}\bar{8}$	14.5	w
67	19.5	w?	$\bar{1}0\bar{1}$	9.0	vw
70	744.9	vs	$\bar{1}0\bar{4}$	6.0	vw
73	31.2	mw	$\bar{1}0\bar{7}$	0.4	vw
76	7.9	vw	$\bar{1}1\bar{0}$	0.4	vvw
$10.\bar{2}$	0.8	a	$\bar{1}1\bar{3}$	7.9	vw
$\bar{5}$	0.4	a	$\bar{1}1\bar{6}$	61.1	m
$\bar{8}$	0.5	a	$\bar{1}1\bar{9}$	39.6	m
$1\bar{1}$	1.2	a	$\bar{1}2\bar{2}$	4.9	vvw
$\bar{1}\bar{4}$	2.0	a	$\bar{1}2\bar{5}$	0.7	vvw
$\bar{1}\bar{7}$	3.3	a	$\bar{1}2\bar{8}$	13.4	vw
$\bar{2}0$	7.9	...	$\bar{1}3\bar{1}$	5.4	vvw
$\bar{2}\bar{3}$	479.6	s	$\bar{1}3\bar{4}$	0.0	vvw
$\bar{2}\bar{6}$	27.0	w	$\bar{1}3\bar{7}$	0.9	vvw
$\bar{2}\bar{9}$	3.0	vvw	$\bar{1}4\bar{0}$	0.9	vvw
$\bar{3}\bar{2}$	1.4	a			

THE MORPHOLOGY OF 141*R*

Because two examples of 141*R* have been discovered it will be necessary to give separate descriptions of each of the specimens.

Crystal No. 109 is blue-gray in color and transparent; it measures about 1.00 mm long, 0.75 mm wide, and 0.25 mm thick. It is tabular parallel to (0001), the two pinacoids being the largest and best developed faces present.

Of the six trigonal pyramid zones, only four have measurable faces, giving goniometer signals of varying quality. There is a striking resemblance between the character of the pyramid faces as observed in the optical goniometer and the reflections of the corresponding 10.*l* planes that exist on x-ray films. In fact a photograph of a series of these goniometer signals would give a fair picture of the 10.*l* reflections observed on a Buerger precession film. Table II is a summary of the various forms observed on the crystal. The quality of the goniometer signal is divided into the two components, intensity and amount of lateral blurring. In attempting a comparison of these data with the x-ray data of Table I or Fig. 1, one should consider the more intense reflections in the cases where two intensities are reported. The goniometer reflections which are much blurred, compare, in general, with the regions on the x-ray film where whole groups of weak or very weak reflections occur. These correspond also with the *clusters* of reflections lying around points *F'*, *B*, and *C* in the graph of calculated 141*R* intensities shown on Fig. 1. The faces which are sharper and of a higher intensity correspond, in general, to reflections on the

TABLE II. Morphological data for SiC type 141*R*.

Form	No. times observed	Quality *I*	Quality Amt. blurred	Angle between form and base Observed	Angle between form and base Calculated[a]
00.1	2	s	none	0°	0°
$10.\bar{1}\bar{2}\bar{2}$	1	vw	much	~47°	47°30′
$10.\bar{1}\bar{1}\bar{9}$	2	w	much	48°16′	48°13′
$10.\bar{1}\bar{1}\bar{6}$	1	vw	much	~48°50′	48°56′
$10.\bar{9}\bar{5}$	2	mw-vvw	some	~54°–54°52′	54°30′
$10.\bar{7}\bar{1}$	3	ms-vvw	none to some	61°45′–62°0′	61°56′
$10.\bar{4}\bar{7}$	3	ms-vvw	some	70°38′–70°52′	70°33′
$10.\bar{2}\bar{6}$?	1	vvw	much	~79°	78°57′
$10.\bar{2}\bar{3}$	3	ms-vvw	some to much	80°0′–80°5′	80°12′
$10.\bar{1}\bar{1}$	1	vw	some	84°57′	85°17′
$10.\bar{8}$	1	vw	much	~85°53′	86°34′
10.0, 10.1	4	w-vw	much	89°48′–~90°	90°00′, 89°34′
10.4?	1	vw	some	88°14′	88°17′
10.16	1	vvw	much	~83°	83°9′
10.19	3	m-vw	much	~82°	81°53′
10.22	3	m-vw	v. much	~80°41′	80°37′
10.25	3	m-vw	some to much	~79°40′	79°22′
10.28	3	vvw	much	~78°	78°7′
10.31	1	vvw	much	~77°	76°54′
10.43	2	vw	some to much	72° 1′–72°7′	72°6′
10.46	4	mw-w	some to much	70°44′–70°53′	70°56′
10.49	2	w-vvw	much	69°38′–~70°	69°48′
10.52	1	vvw	much	68°42′	68°40′
10.70	4	ms-w	none to some	62°15′–62°30′	62°16′
10.73	2	vvw	some	~59°30′	61°16′
10.94	3	ms-mw	some	54°30′–54°53′	54°47′
10.118	1	vw	some	48°15′	48°27′

[a] Calculated from the theoretical axial ratio for a 141 layer cell.

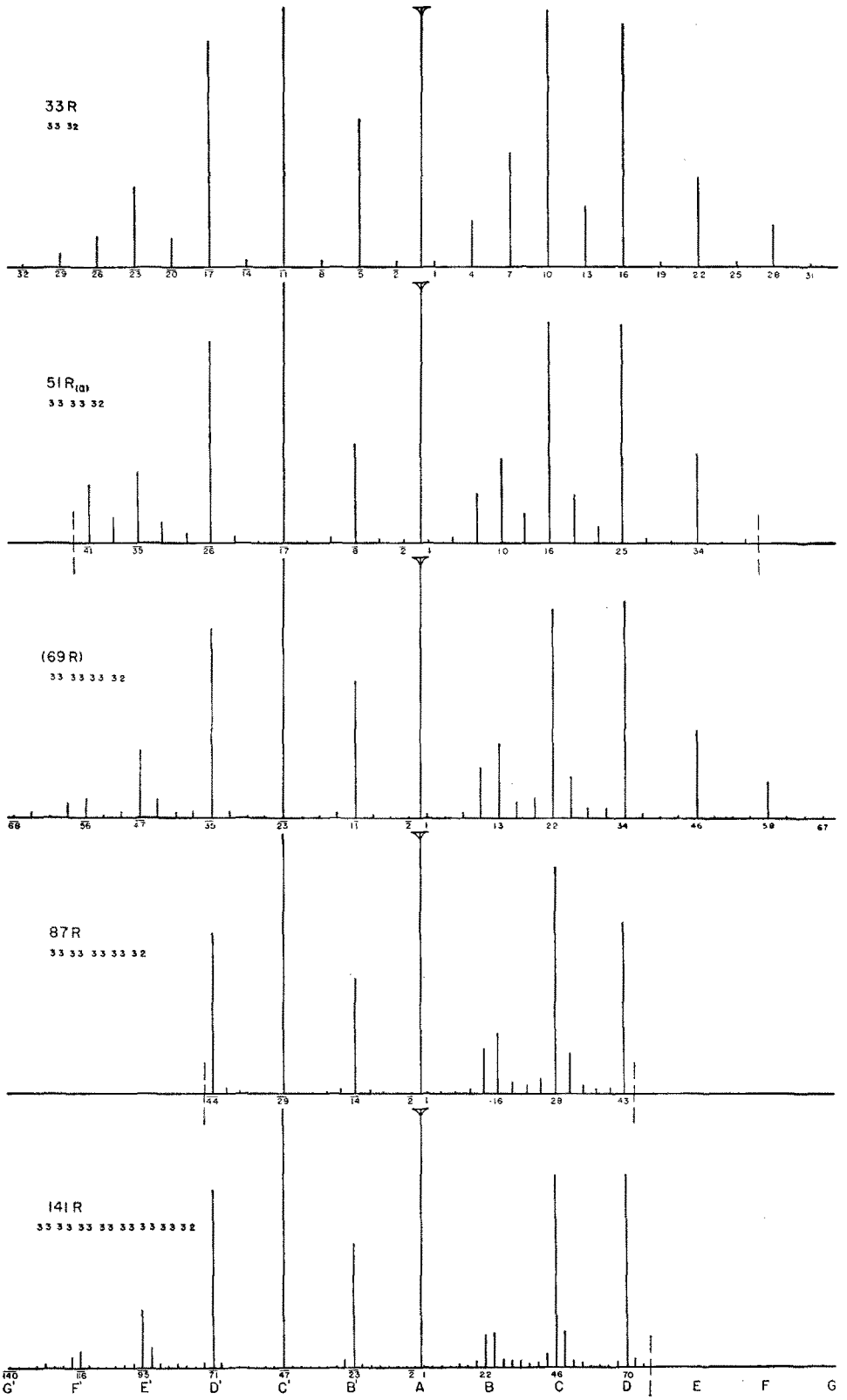

FIG. 1. Comparison of the calculated 10·*l* reflections for five members of the '3...2' series.

x-ray film which are medium strong to very very strong. A study of the morphology revealed that the coalesced $6H$ portion was very minor. Only one pyramid zone showed faces which could definitely be distinguished from the $141R$ faces.

Crystal No. 169 is dark blue in color, translucent, and about 2.5 mm long, 1.5 mm wide, and 0.5 mm thick. It is tabular parallel to (0001). Attached to the edge of this crystal is another silicon carbide plate of about the same size. These two crystals do not appear to be related by twinning. Their c axes are inclined to each other by an angle of about 68°18′ and none of the other axes are parallel. This attached crystal is a combination of types $6H$, $15R$, $33R$ plus a new type which is in the general vicinity of $400H$, if hexagonal, or $1200R$, if rhombohedral. Polymorph $141R$ is also coalesced with $6H$. Of the six trigonal pyramid zones, only four have measurable faces. The measured faces of three of these zones are of very good quality and have angular values indicating pure $6H$. The fourth zone, whose reflections appeared to result from a thinner plate coalesced with the predominant $6H$ portion of the crystal, gave blurred reflections exactly the same in character as those for crystal No. 109 which were summarized above in Table II. It thus appears from the morphology of the crystal that $141R$ is a separate crystal plate syntactically coalesced with a thicker crystal of $6H$.

Crystal No. 169 is also interesting from the point of view that it displays a visible growth spiral. The spiral radiates counterclockwise from the center of the pinacoid on that surface of the crystal which was determined above as being $141R$. Verma[7] who has done considerable work measuring the step heights of the spirals on silicon carbide crystals, has shown that these heights are of a magnitude equal to either fractions or multiples of actual unit cells. The step height of the spiral on $141R$ has not yet been determined. The writer has noticed visible spirals on numerous other specimens of silicon carbide which have giant c_0 values. With the exception of $168R$, he has so far been unable to exactly identify these. Perhaps most crystals of this substance which display spirals visible to the naked eye, possess giant c_0 values. This point definitely warrants further investigation.

TABLE III. The relationship of $6H$ positions to xR $10{\cdot}l$ reflections.

$6H$ $10{\cdot}l$	Fractional relationship	Value of l for the xR $10{\cdot}l$ reflections
$10{\cdot}0$	2/6 way between xR $10{\cdot}1$ and $10{\cdot}\bar{2}$	
$10{\cdot}1$	3/6 way between xR $10{\cdot}l$ and $10{\cdot}l+3$	$l=1+3n$
$10{\cdot}2$	2/6 way between xR $10{\cdot}l$ and $10{\cdot}l+3$	$l=1+3(2n+1)$
$10{\cdot}3$	1/6 way between xR $10{\cdot}l$ and $10{\cdot}l+3$	$l=1+3(3n+2)$
$10{\cdot}4$	Coincides with xR $10{\cdot}l$	$l=1+3(4n+3)$
$10{\cdot}5$	5/6 way between xR $10{\cdot}l-3$ and $10{\cdot}l$	$l=1+3(5n+4)$
$10{\cdot}6$	4/6 way between xR $10{\cdot}l-3$ and $10{\cdot}l$	$l=1+3(6n+5)$
$10{\cdot}\bar{1}$	1/6 way between xR $10{\cdot}l$ and $10{\cdot}l-3$	$l=-(2+3n)$
$10{\cdot}\bar{2}$	Coincides with xR $10{\cdot}l$	$l=-(2+3(2n+1))$
$10{\cdot}\bar{3}$	5/6 way between xR $10{\cdot}l+3$ and $10{\cdot}l$	$l=-(2+3(3n+2))$
$10{\cdot}\bar{4}$	4/6 way between xR $10{\cdot}l+3$ and $10{\cdot}l$	$l=-(2+3(4n+3))$
$10{\cdot}\bar{5}$	3/6 way between xR $10{\cdot}l+3$ and $10{\cdot}l$	$l=-(2+3(5n+4))$
$10{\cdot}\bar{6}$	2/6 way between xR $10{\cdot}l+3$ and $10{\cdot}l$	$l=-(2+3(6n+5))$

[7] A. R. Verma, Nature **168**, 431 (1951); Z. Elektrochem. **56**, 4, 268 (1952).

141R AND OTHER SIMILAR SILICON CARBIDE STRUCTURES

The $141R$ zigzag sequence falls into the '3...2' rhombohedral series proposed by Ramsdell,[1] where the ratio of 33's to 32's in this case is 7:1. The following extension of the Ramsdell series includes this new form:

		Ratio of 33 to 32
$15R$	32	0:1
$33R$	3332	1:1
$51R_{(a)}$	333332	2:1
$(69R)$‡	33333332	3:1
$87R$	3333333332	4:1
$(105R)$‡	333333333332	5:1
$(123R)$‡	33333333333332	6:1
$141R$	3333333333333332	7:1
$6H$	33333333333333333...∞	1:0

These sequences must be repeated three times to give the complete unit cell, since the last layer must be directly above the initial layer. Each member of this series (xR) will have

$$x=3(6n+5) \qquad (1)$$

where x=number of layers in the polymorph, n is any whole number, $6=3+3$, and $5=3+2$.

Ramsdell[1] has pointed out that major "blocks" of the larger cells have the $6H$ structure because of the increasing number of successive 33 units in the zigzag sequence, and thus the larger cells in the series become increasingly more like $6H$. $6H$ is the limiting case of this series. Because of the abundance of the 33 units in the many-layered rhombohedral structures, the intensities of the rhombohedral $10.l$ reflections lying near $6H$ $10.l$ positions should be greater.

Because every polymorph of silicon carbide has the same a axis and a c axis whose length is an exact multiple of a common unit ($d=2.513$ kX), there is a coincidence of the rows of $10.l$ reflections of all silicon carbide types. Moreover, the *range* from 10.0 to $10.x$ for every xR or xH type will be equal on a film. This distance corresponds to the reciprocal of the basic unit. This relationship between $6H$ and $141R$ was used above to identify the $141R$ form. In the following discussion

‡ These types have not yet been discovered.

xR 10.l reflections which fall in this *range* will simply be called xR reflections. The 6H 10.l reflections will be designated 6H positions since we are only interested in their position on the films in relationship to actual xR reflections.

It was stated above that the rhombohedral 10.l reflections lying near 6H 10.l positions should be of greatest intensity. In order to determine which xR reflections are most influenced by these 6H positions it is necessary to determine which of the 10.l reflections for the members of the '3...2' series are most closely related to these 6H positions. Table III summarizes the relationship of 13 6H 10.l positions to their two neighboring xR 10.l reflections. The value n, used in determining l for the 10.l reflections, can be found from $n=(x-15)/18$, a rearrangement of Eq. (1) above. In Table III it is easily observed that the 6H positions are related to the xR reflections in a limited number of ways. The 6H position can either coincide with a xR reflection or be 1/6, 2/6, 3/6, 4/6, or 5/6 the way between two of the xR reflections. The importance of these different fractions will be discussed in more detail later using 141R as an example.

The general effect of the 6H positions of the xR reflections is easily observed in Fig. 1 which is a graph showing a comparison of the calculated 10.l reflections for 5 members of the '3...2' series. A, B, C, D, E, F, and G are the locations of the 6H positions 10.0, 10.1, 10.2, etc. respectively, and B', C', D', E', F', and G' are the locations of the 6H positions $10.\bar{1}$, $10.\bar{2}$, etc., respectively.

Those calculated intensity values plotted in Fig. 1 for type 141R are the same as those listed in Table I. The values for 33R, 51$R_{(a)}$, 87R§ were taken from Ramsdell.[1,8] Type 69R has not yet been discovered, so no intensity values for this structure have previously been published. The complete *ranges* of 10.l reflections for 51$R_{(a)}$, 87R, and 141R have not been calculated. For this reason the extent of their calculation is indicated by the light vertical dashed lines in the figure. The darkest 10.l reflections, which in each case have l equal to 1/3.x of the xR form were arbitrarily made equal for each of the types.

The intensity of a xR reflection is not only conditioned by its promixity to a 6H 10.l position, but also depends upon the intensity of the 6H reflection that falls at this position. In other words a xR reflection falling near a very intense 6H reflection position should itself be of a high intensity, and a xR reflection next to a weak 6H reflection position should itself be weak.

In order to show more clearly the dual importance of the proximity as well as the intensity of a 6H position, the relative intensities of the 6H positions are compared to the relative intensities of the neighboring 141R reflections in Table IV. For convenience the intensities for 6H $10.\bar{2}$ and 141R $10.\bar{4}\bar{7}$ were made equal, because they are the most intense reflections for both polymorphs and coincide with each other in position. On this basis their magnitudes are in such good agreement, that a good comparison is possible.

TABLE IV. Intensities of 6H reflections compared to adjoining 141R reflections.

6H 10.l	6H intensity	Adjoining 141R reflections	141R intensity	Fractional distance of 6H between 141R
10.0	0.0	10.1 –$10.\bar{2}$	0.8–0.8	2/6
10.1	478.1	10.22 –10.25	190.3–129.9	3/6
10.2	1000.0	10.46 –10.49	740.4–139.3	2/6
10.3	640.5	10.70 –10.73	744.9–31.2	1/6
10.4	311.2	10.94	not calc.	coincides
10.5	129.5	10.115–10.118	not calc.	5/6
10.6	0.0	10.139–10.142	not calc.	4/6
$10.\bar{1}$	478.1	$10.\bar{2}\bar{3}$ –$10.\bar{2}\bar{6}$	479.6–27.0	1/6
$10.\bar{2}$	1000.0	$10.\bar{4}\bar{7}$	1000.0	coincides
$10.\bar{3}$	640.5	$10.\bar{6}\bar{8}$ –$10.\bar{7}\bar{1}$	18.3–685.8	5/6
$10.\bar{4}$	311.2	$10.\bar{9}\bar{2}$ –$10.\bar{9}\bar{5}$	78.0–221.3	4/6
$10.\bar{5}$	129.5	$10.\bar{1}\bar{1}\bar{6}$–$10.\bar{1}\bar{1}\bar{9}$	61.1–39.6	3/6
$10.\bar{6}$	0.0	$10.\bar{1}\bar{4}\bar{0}$–$10.\bar{1}\bar{4}\bar{3}$	0.9–not calc.	2/6

It is easily noticed that in the cases where a 6H position is 1/6 or 5/6 the way between two 141R reflections (e.g., 6H $10.\bar{1}$), the intensity of that 141R reflection nearest the 6H position is the greater by a large ratio. Its intensity is close to the intensity of the 6H reflection its neighbors. When a 6H position is 2/6 or 4/6 the way between two 141R reflections (e.g., 6H $10.\bar{4}$) the intensity of that 141R reflection nearest the 6H position is the greater, but by a smaller ratio than for the 1/6 or 5/6 case. Also its intensity is considerably less than that of the neighboring 6H reflection. When the 6H position is 3/6 way between two 141R reflections (e.g., 6H $10.\bar{5}$ and 10.1) both of these reflections will have an intensity much less than the 6H intensity and will differ from each other by a very small ratio. In the cases where a 141R reflection lies in the same position as a possible 6H reflection (e.g., 141R $10.\bar{4}\bar{7}$) it will have an intensity nearly equal to that corresponding 6H reflection. The intensities of the other 141R reflections neighboring this case (e.g., 141R $10.\bar{4}\bar{4}$ and $10.\bar{5}0$) are much smaller.

In the discussion above, only the influences of the 6H positions upon two neighboring xR reflections were considered. These effects can be somewhat more generalized in considering the other xR reflections. If one temporarily disregards the reflections of high intensity discussed above and considers the remaining reflections (Fig. 1), it will be noticed that in the regions between G' and D' and also between A and D, there are *clusters* of reflections of a higher intensity compared to the remaining regions. More specifically, they lie as *clusters* around 6H $10.\bar{5}$, $10.\bar{4}$, 10.1, and 10.2. These are regions where the 6H positions are related to xR reflections by 2/6, 3/6, and 4/6 as was discussed earlier. When the 6H

§ Upon recalculation it was shown that $10.\bar{2}\bar{9}$ for 87R should be more intense than the 10.28 reflection. The reverse condition had previously been reported.

[8] L. S. Ramsdell, Am. Mineralogist **30**, 519 (1945).

positions superimpose, or are very close to xR reflections, e.g., by 1/6 or 5/6, the adjoining neighbors are very low in intensity or nearly absent. An example of this is the neighbors of $141R$ $10.\overline{47}$ in Fig. 1. The xR reflections in regions corresponding to the $6H$ missing reflections 10.0, 10.6, and $10.\bar{6}$ are themselves usually very weak or absent.

Another important relationship exists between the members of the series in discussion. As the number of layers in the form increases the ratio between the intense reflections near $6H$ positions and those *clusters* of less intense reflections also increases. This is easily understood when one recalls that in the larger cells of the series the number of 33 units in the zigzag sequence increases, making the structure more like $6H$ in character. As the structure approaches this limiting case, the reflections near $6H$ positions will become more intense while other reflections become less intense. When $6H$ is reached only the $6H$ positions are present. As a result of this fact it is obvious that above a certain point the many-layered forms in the series would have no distinguishing characteristics. Only reflections next to $6H$ positions would be noticeable on the film. This increasing ratio between the more intense reflections and the less intense reflections makes intensity evaluation very difficult in the many-layered forms. Those intense reflections near $6H$ positions have to be greatly overexposed before the less intense *clusters* of reflections can be observed or evaluated. These facts were considered in the evaluation of the $141R$ intensities in Table I.

In résumé it may be said that all xR forms belonging to the '3...2' series have the following characteristics: (a) x must equal $3(6n+5)$. (b) $10.l$ reflections lying next to $6H$ positions have the greatest intensity. In general, the intensity of these depends upon the exact proximity of the $6H$ position and upon the intensity of the possible $6H$ $10.l$ at that position. (c) All of the remaining xR reflections follow a characteristic pattern, in that they fall as *clusters* of reflections of medium intensity around the $6H$ $10.\bar{5}$, $10.\bar{4}$, 10.1, and 10.2 positions. (d) As the number of layers in the form increases there is an increasing ratio between the intensity of the reflections near $6H$ positions and the intensity of the *clusters* of less important reflections.

It seems logical to conclude that any new type which fits all of the above conditions would belong to this series.

SILICON CARBIDE TYPE 393R

Silicon carbide type $393R$, which was discovered during the course of the writing of this paper, serves as an excellent example of the usefulness of the above study of the '3...2' series. The fact that the crystal was coalesced with type $6H$ permitted its unambiguous identification using Laue photographs.

Of great importance is the fact that this type fits the condition $x=3(6n+5)$, where $n=21$. Buerger precession films showed the characteristic intensity distribution for the '3...2' series. As was to be expected, the reflections next to $6H$ positions were so intense, compared to the minor *clusters* of reflections, that at first glance the crystal appeared to be pure $6H$. Closer inspection, however, showed the presence of those less intense *clusters* of reflections in the regions characteristic for them in this series.

Consequently, on the basis of empirical reasoning, it seems quite certain that $393R$ is a member of the '3...2' series. Its zigzag sequence is 3333333333333333-33333333333333333333333333332, where the ratio of 33's to 32's is 21:1. There is no point in listing the coordinates of the 786 atoms in the unit cell of this form, since they can easily be derived from the above zigzag sequence.

This new rhombohedral polymorph has the following (hexagonal) cell dimensions:

$$a_0=3.073\ kX,\quad c_0=987.60_9\ kX,\quad Z=393,$$

or, for rhombohedral axes,

$$a_{rh}=329.20_8\ kX,\quad \alpha=0°32',\quad Z=131.$$

The space group for $393R$ is $R3m$, as in the other rhombohedral polymorphs.

The crystal is dark blue in color, almost opaque, and about 2.5 mm long, 1.5 mm wide, and 1.0 mm thick. X-ray data show that it is syntactically coalesced with $6H$. An unusual feature of the crystal is the fact that it is also coalesced with another $6H$ crystal in such a manner that their c axes are parallel but their a axes have an angle between them of about 3°19′. The crystal is also randomly attached to other bits of various silicon carbide crystals which have not been identified. One basal pincoid of $393R$ shows a pattern of concentric scalloped-circles. It was because of this unusual surface feature that the crystal was initially investigated. Four of the six trigonal pyramid zones have measurable faces. The measured angles showed no appreciable departure from the corresponding $6H$ angles. This is to be expected since the structure is so closely related to $6H$. Most of the reflections were of good quality. Because of the very close similarity of this crystal to $6H$ it does not seem necessary to include a table of morphological data.

CONCLUSION

Virtually this study provides an empirical mechanism for the direct determination of the structures of an evidently common group of silicon carbide polymorphs. Perhaps from now on the tedious calculations involved in the determination of the intensities of the many-layered forms of the '3...2' series can be eliminated. Similar studies of other series of silicon carbide zigzag sequences might prove as equally useful in the solution of the structures of other many-layered types.

ACKNOWLEDGMENTS

This investigation was carried out through the financial assistance of the U. S. Office of Naval Research.

The writer wishes to thank Professor L. S. Ramsdell of the Mineraological Laboratory, University of Michigan, for his many helpful suggestions during the progress of the study. Special mention is also due Dr. J. A. Kohn, U. S. Bureau of Mines, Electrotechnical Laboratory, Norris, Tennessee, who began the study of type 141*R* in 1950. The following, of the University of Michigan, should also be acknowledged for their help with the intensity calculations: W. B. Fauser, Jr., J. Funkhouser, A. A. Giardini, and E. L. Hastings.

THE JOURNAL OF CHEMICAL PHYSICS VOLUME 22, NUMBER 12 DECEMBER, 1954

Vibrational Spectra of $CF_2=CHD$ and $CF_2=CD_2$*

WALTER F. EDGELL AND CASPER J. ULTEE†
Department of Chemistry, Purdue University, Lafayette, Indiana
(Received May 14, 1954)

A method has been devised to prepare $CF_2=CD_2$ and $CF_2=CHD$. The infrared spectra of the gaseous compounds and the Raman spectra of the liquids have been determined. The observed frequencies have been assigned to the fundamental modes of vibration and to overtones and combinations. The torsional frequency has been estimated as *ca* 720 and *ca* 520 cm^{-1} in $CF_2=CH_2$ and $CF_2=CD_2$, respectively. The overtone of the torsional frequency interacts with the CH_2 or the CD_2 deformation fundamental and this is the cause of the anomalous results with the product rule.

INTRODUCTION

THE infrared spectrum of $CF_2=CH_2$ was first studied by Torkington and Thompson in 1945.[1] Edgell and Byrd reported the Raman spectrum of liquid $CF_2=CH_2$ in 1949 and assigned the fundamentals.[2] At about the same time Smith, Nielsen, and Claassen published the results of their investigation of the Raman and infrared spectrum of gaseous $CF_2=CH_2$.[3] In general, there is good agreement between the last two investigations, except for the assignment of the A_1 CH_2 deformation frequency and the A_2 torsion.

This laboratory has been studying the coupling between the (hypothetical) group and skeletal motions during the actual fundamental vibrations of some simple molecules. $CF_2=CH_2$ is quite interesting from this point of view. However, isotopic species are needed for a complete analysis. These and other reasons have prompted us to investigate the spectra of $CF_2=CD_2$ and $CF_2=CHD$. It was also hoped that such a study might remove the uncertainties in the $CF_2=CH_2$ assignment. No previous references to these molecules have been found.

PREPARATION OF SAMPLES

The $CF_2=CD_2$ was prepared by the following reactions:

(1) $CF_3CD_2OH+ClSO_2$—⟨⟩—$CH_3\rightarrow$

$CF_3CD_2OSO_2$—⟨⟩—CH_3+HCl;

(2) $CF_3CD_2OSO_2$—⟨⟩—$CH_3+NaI\rightarrow$

$CF_3CD_2I+NaOSO_2$—⟨⟩—CH_3;

(3) $CF_3CD_2I+Mg\rightarrow CF_2=CD_2+MgIF$.

The CF_3CD_2OH was prepared by the method of Henne *et al.* using $LiAlD_4$ instead of $LiAlH_4$,[4] and following the procedure of Edgell and Borneman.[5] The alcohol was converted to the *p*-toluenesulfonic acid ester, a typical preparation of which is given below:

50 g (0.5 mole) of CF_3CD_2OH were mixed with 105 g (0.55 mole) of $ClSO_2$⟨⟩CH_3 in a 1-liter flask provided with a reflex condenser, stirrer, and dropping funnel. The flask was cooled in an ice bath and 80 g (~1 mole) of pyridine were added slowly. The reaction mixture was stirred overnight at a temperature of 0°C. The resulting mixture was poured on ice and neutralized with dilute HCl. The ester was filtered off, washed with water, recrystallized from petroleum ether, and

* Abstracted from the Ph.D. thesis of C. J. Ultee, Purdue University, April, 1954.

† Purdue Research Foundation Fellow, 1952–1953 and Standard Oil Foundation, Inc., Fellow 1953–1954.

[1] P. Torkington and H. W. Thompson, Trans. Faraday Soc. **41**, 236 (1945).

[2] W. F. Edgell and W. E. Byrd, J. Chem. Phys. **17**, 740 (1949); **18**, 892 (1950).

[3] Smith, Nielsen, and Claassen, J. Chem. Phys. **18**, 326 (1950).

[4] Henne, Alm, and Smook, J. Am. Chem. Soc. **70**, 1968 (1948).

[5] W. F. Edgell and E. H. Borneman, to be published. See also E. H. Borneman, Ph.D. thesis, Purdue University, 1952.